Key structural motifs in PY-nuclear localization signals enable inhibitor design for a nuclear import pathway

Ahmet E. Cansizoglu[1], Brittany J. Lee[1], Zi Chao Zhang[1], Beatriz Fontoura[2] and Yuh Min Chook[1].

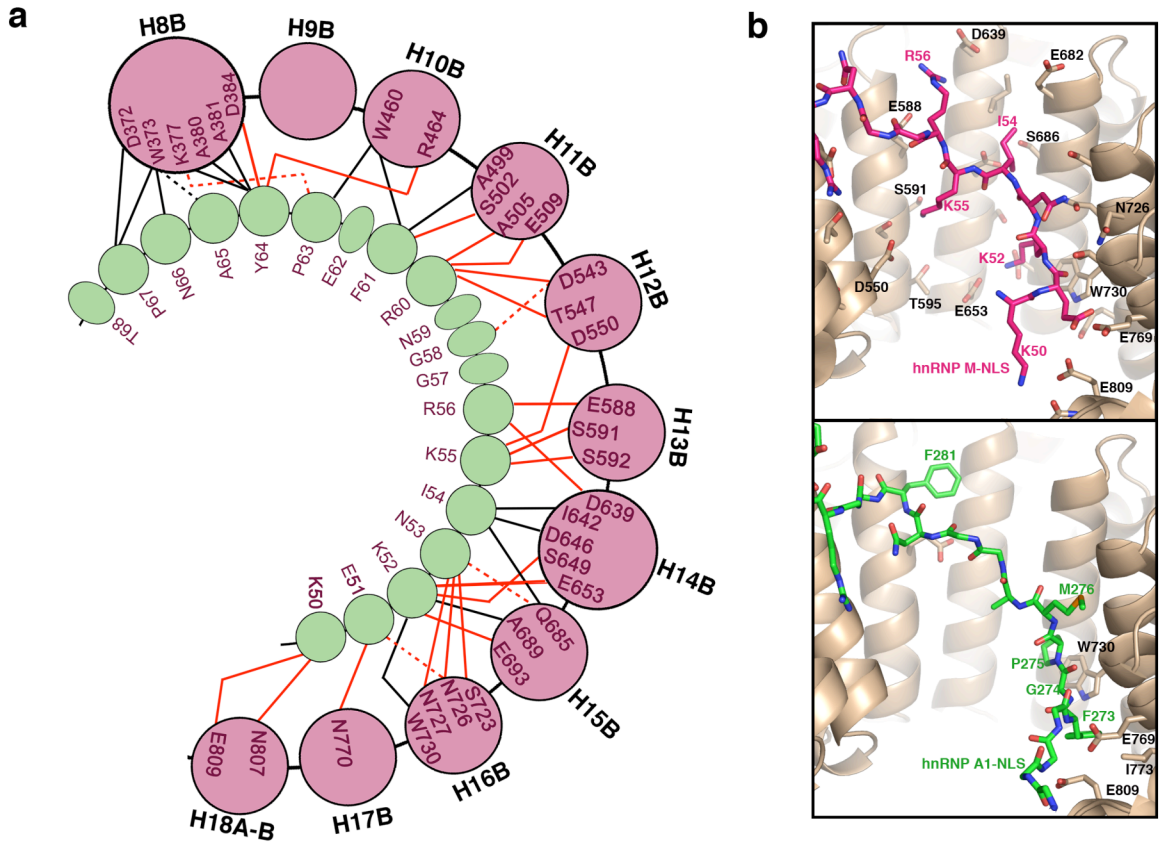

Supplementary Figure 1. Interactions between hnRNP M-NLS and Kapβ2.
(a) Kapβ2-hnRNP M-NLS contacts (< 4.0 Å). hnRNP M-NLS residues are shown as green circles and Kapβ2 helices as pink circles. Contacts involving the main chain and sidechains of hnRNP M-NLS are shown with dashed and solid lines, respectively. Hydrophobic contacts are in black and polar contacts in red. **(b)** Interactions between Kapβ2 (light brown) and the N-terminal NLS motifs of hnRNP M (magenta) and A1 (green).

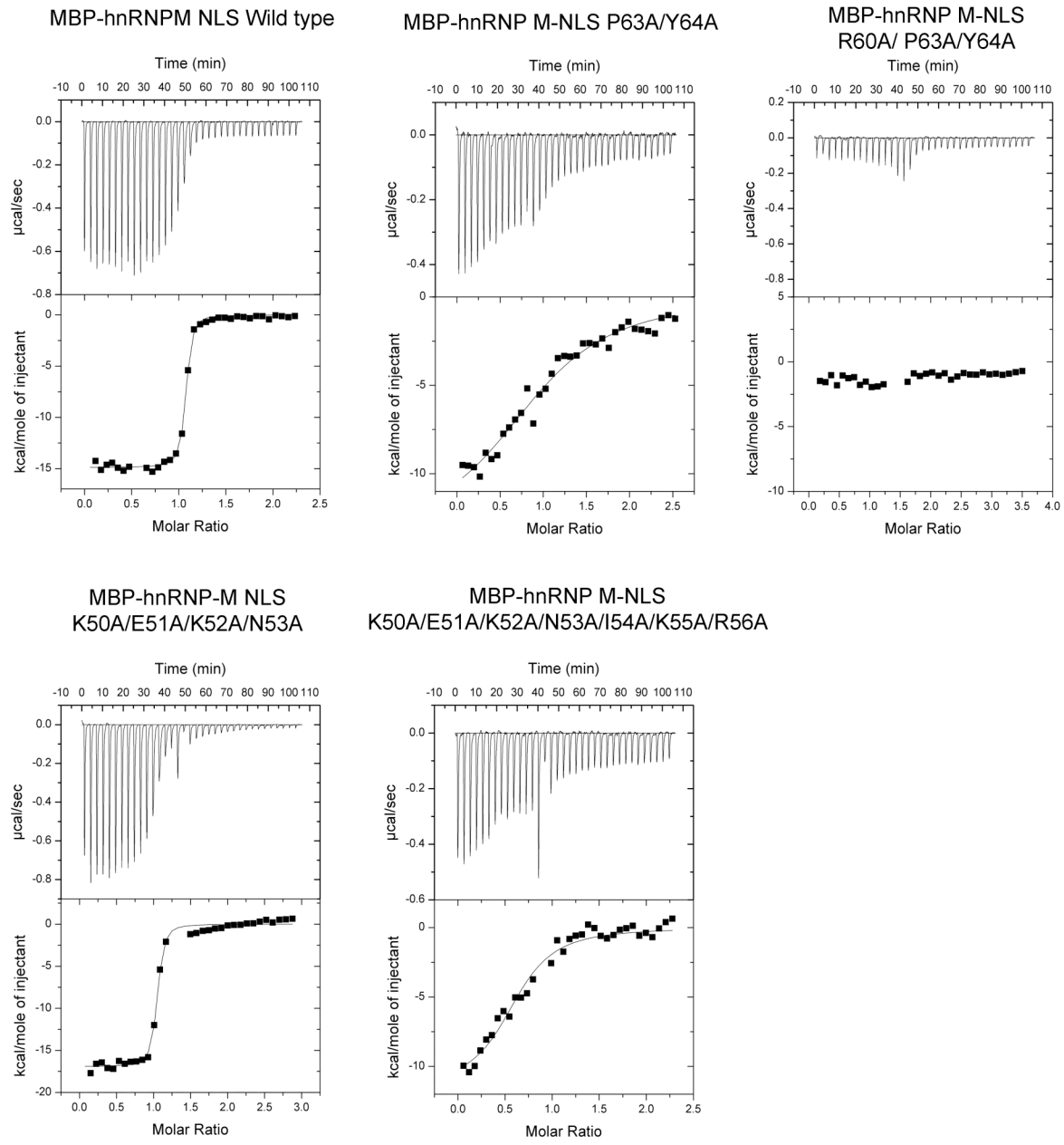

Supplementary Figure 2. Isothermal Titration Calorimetry (ITC) measurements of select hnRNP M-NLSs binding to Kapβ2.

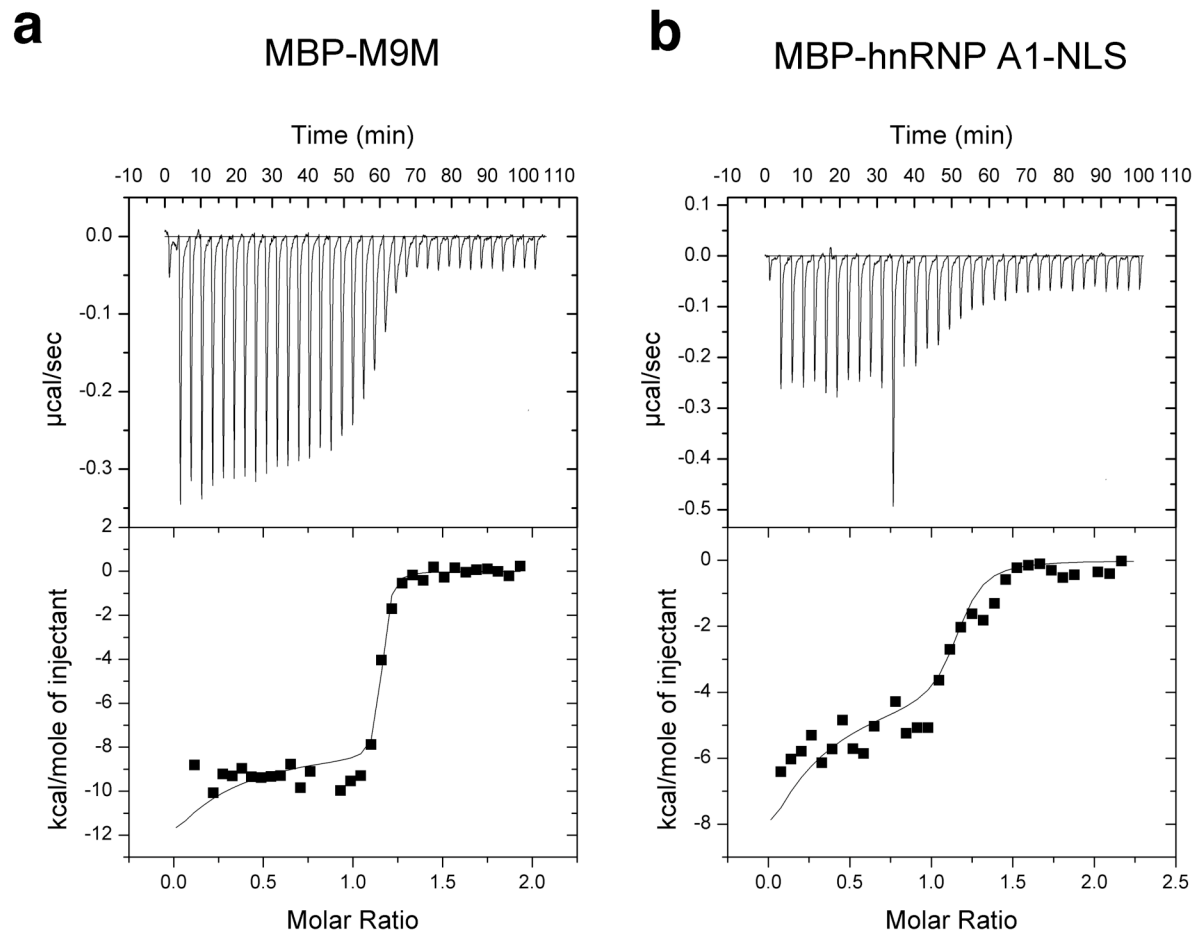

Supplementary Figure 3. Competition ITC data for inhibitor MBP-M9M binding to Kapβ2.

(a) The calorimetry cell containing 12 µM Kapβ2 and 18 µM R284A/P288A/Y289A mutant of MBP-hnRNP A1-NLS was titrated with syringe solution containing 108 µM MBP-M9M inhibitor. The K_D obtained for Kapβ2-M9M interaction is 107 pM. **(b)** A control experiment was performed with 12 µM Kapβ2 and 20 µM R284A/P288A/Y289A mutant of MBP-hnRNP A1-NLS in the calorimetry cell, and titration with syringe solution of 154 µM of MBP-hnRNP A1-NLS. The K_D obtained for Kapβ2-hnRNP A1-NLS interaction by ITC competition is 20 nM, comparable to K_D of 42 nM by direct/standard ITC.

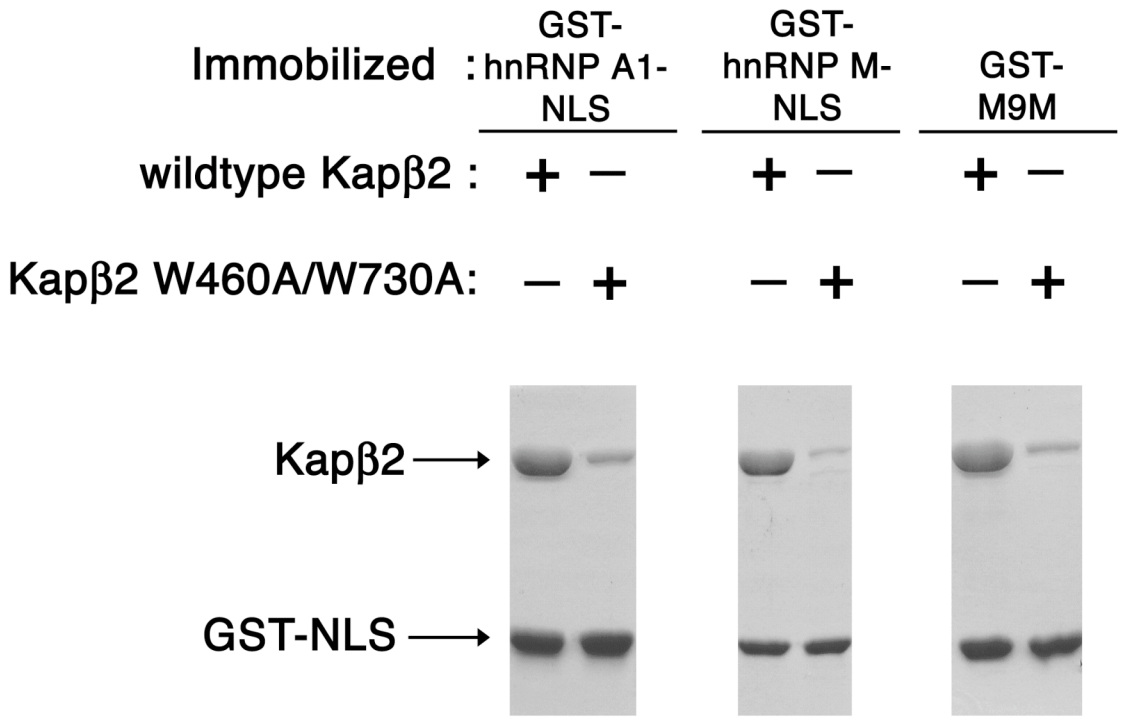

Supplementary Figure 4. M9M, hnRNP M-NLS and hnRNP A1-NLS bind to the same site on Kapβ2.

Immobilized GST-fusions of hnRNP A1-NLS, hnRNP M-NLS and inhibitor M9M all show significantly decreased binding to Kapβ2 W460A/W730A mutant. Residue W460A of Kapβ2 contacts the C-terminal PY motif of the PY-NLSs whereas W730A contacts both the N-terminal hydrophobic motif of hnRNP A1 hPY-NLS and the N-terminal basic motif of the hnRNP M bPY-NLS.

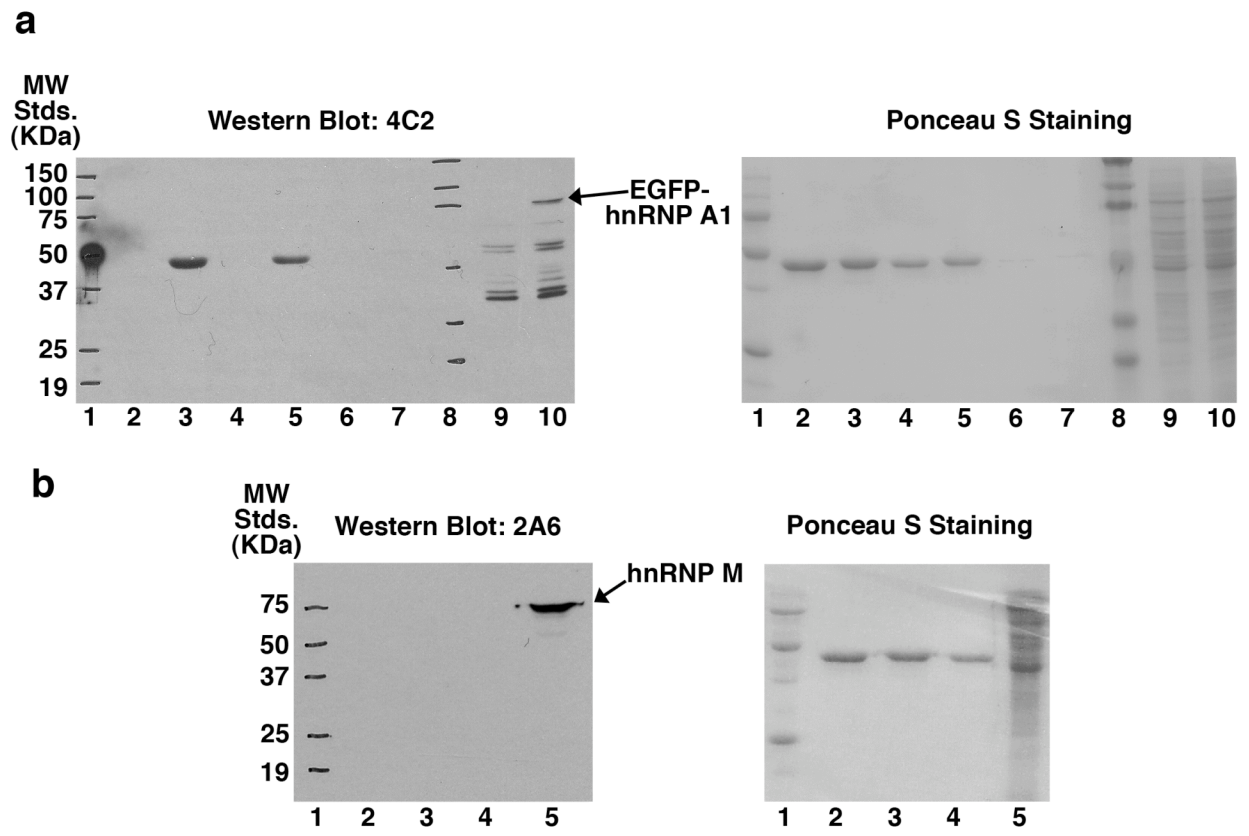

Supplementary Figure 5. Western blots using antibodies against hnRNPs A1 and M.

(a) Western Blot with antibody 4C2 (left), which recognizes human hnRNPs A1, A2 and B1, and visualization of proteins by Ponceau staining (right). Lanes 2, 4 and 6 contain 2 ug, 1 ug, and 0.1 ug of MBP-M9M; lanes 3, 5 and 7 contain 2 ug, 1 ug and 0.1 ug of MBP-hnRNP A1-NLS; Lane 9 contains control HeLa cell lysate and lane 10 has lysate from myc-EGFP-A1-transfected HeLa cells. Lanes 1 and 8 are molecular weight standards.

(b) Western Blot with antibody 2A6 (left), which recognizes human hnRNP M, and visualization of proteins by Ponceau staining (right). Lane 1 contains molecular weight standards; Lane 2 contains 1 ug of MBP-M9M; Lane 3 contains 1 ug of MBP-hnRNP A1-NLS; Lane 4 contains 1 ug of MBP-hnRNP M-NLS; Lane 5 contains Hela cell lysate.

Key structural motifs in PY-nuclear localization signals enable inhibitor design for a nuclear import pathway

Ahmet E. Cansizoglu[1], Brittany J. Lee[1], Zi Chao Zhang[1], Beatriz Fontoura[2] and Yuh Min Chook[1].

Supplementary Table 1. Data collection and refinement statistics

	Kapβ2-hnRNP M-NLS
Data collection	
Space group	C2
Cell dimensions	
a, *b*, *c* (Å)	153.2, 155.0, 141.5
α, β, γ (°)	90.0, 92.6, 90.0
Resolution (Å)	50-3.0(3.1-3.0)*
R_{sym} or R_{merge}	0.068 (0.65)
$I / \sigma I$	20 (1.5)
Completeness (%)	98.8 (92.3)
Redundancy	3.6 (3.1)
Refinement	
Resolution (Å)	50-3.1
No. reflections	56,210
R_{work} / R_{free}	0.255/0.290
No. atoms	
Protein	12,802
Ligand/ion	
Water	
B-factors	Kapβ2 Chain A: 90.4 Å^2 Kapβ2 Chain B: 95.9 Å^2 hnRNP M-NLS chain C: 102.7 Å^2 (51-58: 127.9 Å^2, 59-64: 81.4 Å^2, 65-68: 101.8 Å^2) hnRNP M-NLS chain D: 117.4 Å^2 (49-58: 149.8 Å^2, 59-64: 75.9 Å^2, 65-69: 120.6 Å^2)
Protein	
Ligand/ion	
Water	
R.m.s deviations	
Bond lengths (Å)	1.197
Bond angles (°)	0.008

*Highest resolution shell is shown in parenthesis.

Supplementary Table 2

Kap β2 binding to hnRNP M NLS and mutants: Dissociation Constants Measured by Isothermal titration calorimetry

MBP-hnRNP M(41-70)	K_D
Wild type	10± 1.7 nM
K50A	16.4 ± 0.4 nM
K52A	14.6 ± 0.3 nM
N53A	17.1 ± 0.5 nM
I54A	8.8 ± 1.8 nM
K55A	7.6 ± 2.3 nM
R56A	13.9 ± 2 nM
K50A/E51A/K52A/N53A	22.3 ± 4.1 nM
K50A/E51A/K52A/N53A/I54A/K55A/R56A	1.2 ± 0.2 μM
F61A	11.2 ± 1.6 nM
P63A/Y64A	4.5 ± 0.7 μM
F61A/ P63A/Y64A	8.6 ± 1.4 μM
R59A/ P63A/Y64A	ND
P67A	8.7 ± 1.5 nM

Key structural motifs in PY-nuclear localization signals enable inhibitor design for a nuclear import pathway

Ahmet E. Cansizoglu[1], Brittany J. Lee[1], Zi Chao Zhang[1], Beatriz Fontoura[2] and Yuh Min Chook[1].

[1] Department of Pharmacology, University of Texas Southwestern Medical Center at Dallas, 6001 Forest Park, Dallas, TX 75390-9041, U.S.A.

[2] Department of Cell Biology, University of Texas Southwestern Medical Center at Dallas, 5323 Harry Hines Blvd., Dallas, TX 75390-, U.S.A.

Supplementary Methods

Protein expression, purification and complex formation

Human Kapβ2 (accession AAB58254) was expressed in pGEX-Tev vector (pGEX-4T3 (GE Healthcare, UK) with a Tev cleavage site) as a GST fusion protein and purified as previously described[1]. Residues 337-367 of Kapβ2 were replaced with a GGSGGSG linker to obtain diffracting crystals. This truncation does not interfere with NLS binding. The NLS for human hnRNP M (accession NM_005968) was expressed in BL21(DE3) *E. coli* cells as a GST-fusion protein spanning residues 41-70, and purified as described previously described[2]. GST-hnRNP M-NLS was mixed with Kapβ2 in a 3:1 molar ratio, treated with Tev protease and the resulting complex purified by gel filtration chromatography. The complex was concentrated to 20 mg/ml for crystallization.

NLS mutants were obtained by site directed mutagenesis using Quickchange (Stratagene, La Jolla, CA). Nucleotide sequencing was performed on all mutants. For ITC measurements, NLS wild type and mutant fragments were expressed as fusion proteins in pMAL-Tev vector

(pMAL (New England Biolabs, UK) with Tev site). Expression and purification were similarly previous studies[1].

Crystallization, data collection and structure determination

Kapβ2-hnRNP M-NLS complex was crystallized by vapor diffusion using 100 mM HEPES pH 7.0, 2.7 M potassium formate and 10% glycerol in the reservoir solution. Crystals were flash frozen in liquid propane. 3.0 Å data from these crystals were collected at beamline 19-ID at the Advanced Photon Source, Argonne National Laboratory at X-ray wavelength 12.66 keV and temperature 100 K. Data was processed using HKL2000[3]. Kapβ2-hnRNP M-NLS crystals were in a very similar space group as the Kapβ2-hnRNP A1-NLS crystals (PDB ID: 2h4m [1]), with space group C2, unit cell parameters a=152.0 Å, b=154.1 Å, c=141.7 Å and β=91.7° and two complexes in the asymmetric unit. The Kapβ2-hnRNP A1-NLS model was used as a search model for molecular replacement using the program Phaser[4]. Positional refinement using REFMAC5[5] followed by solvent flipping using CNS[6] yielded electron density maps that allowed ~98% of the model to be built using Coot[7]. The density was further improved using rigid body, positional and simulated annealing refinement of Kapβ2 alone, with programs in CNS[6]. The same test data set was used throughout the entire refinement process. The Fo-Fc map plotted at 2.5σ shows interpretable density for hnRNP M-NLS residues 49-53 and 55-68 in complex I, and residues 49-69 in complex II. The final refined model shows good stereochemistry with R_{factor} of 26.3% and R_{free} of 29.4%. Ramachandran plot for final model: 90.7% in most favored and 9.3% in allowed regions. Fig. 1a-b and Supplementary Fig. 1b were drawn using PYMOL[8].

Quantitation of binding affinity with Isothermal Titration Calorimetry

Binding affinities for wild type and mutant MBP-hnRNP M-NLS were determined using Isothermal titration calorimetry (ITC). The experiments were performed using a MicroCal Omega VP-ITC calorimeter (MicroCal Inc., Northampton, MA). MBP-NLS proteins were dialyzed against buffer containing 20 mM Tris pH 7.5, 100 mM NaCl and 2 mM β-mercaptoethanol. 100-300 μM Wild type and mutant MBP-hnRNP A1-NLS proteins were titrated into the sample cell containing 10-100 μM full-length Kapβ2. All ITC experiments were done at 20°C with 35 rounds of 8 μl injections. Data were plotted and analyzed using the single binding site model of MicroCal Origin software version 7.0.

Direct titration of ligand to protein in ITC reliably measures K_D values in the 10^{-8} to 10^{-3} M range. hnRNP A1-NLS and hnRNP M-NLS bind Kapβ2 at the lower limit of this K_D range (K_D of 42 nM and 10 nM respectively, by standard ITC[1]). Since the inhibitory M9M peptide appears to bind Kapβ2 with higher affinity than the natural NLSs (Figs. 2a-c), we performed competition ITC to extend the range of measurable tight ($K_D < 10^{-9}$ M) affinities. hnRNP A1-NLS R284A/P288A/Y289A mutant (K_D of 461 nM, measured by standard ITC[1]) was used as the competition displacement ligand. The calorimetry cell containing 12 μM Kapβ2 and 18 μM R284A/P288A/Y289A mutant of MBP-hnRNP A1-NLS was titrated with syringe solution of 108 μM MBP-M9M inhibitor (or 154 μM wildtype hnRNP A1-NLS as control). The experiment was repeated using 20 μM of the competition displacement ligand. Data were analyzed with the competition model in MicroCal Origin software version 7.0 to give K_D values of 107 pM and 111 pM for M9M and K_D of 20 nM for wildtype hnRNP A1-NLS (Supplementary Fig. 3).

Qualitative Binding assays

RanGTP-mediated dissociation experiments: approximately 20-40 μg of GST-hnRNP A1-NLS, GST-hNRNP M-NLS and GST-M9M were immobilized on glutathione sepharose

(Amersham, NJ, USA). 20 μg of Kapβ2 was added to the peptide bound sepharose for 10 minutes followed by extensive washing (TB Buffer: 20 mM HEPES pH7.3, 110 mM KAc, 2 mM DTT, 2 mM MgAc, 1 mM EGTA and 20% Glycerol). A second incubation was done with increasing concentrations of RanGTP (0.32 μM, 0.64 μM, 0.96 μM, 1.28 μM, 1.6 μM), each in 100 μL solution. After extensive washing, a quarter of the bound proteins were separated by SDS-PAGE and visualized with Coomassie staining.

Competition NLS dissociation experiments: approximately 20-40 μg of GST-hnRNP A1-NLS was immobilized on glutathione sepharose (Amersham, NJ, USA) and incubated with 10 μg of Kapβ2 and 7 μg of either MBP-hnRN M-NLS, MBP-hnRNP A1NLS or MBP-M9M. Samples were washed extensively and a quarter of each reaction was subjected to SDS-PAGE and Coomassie staining.

Kapβ1 binding experiments: approximately 1 μg GST-Kapβ1 immobilized on glutathione sepharose (Amersham, NJ, USA) and incubated with Kapα (5 μg), Kapα (5 μg) and IBB-His_6 (~50 μg), Kapα (5 μg) and MBP-M9M (7 μg) or MBP-M9M (7 μg). Samples were washed extensively and a quarter of each reaction was subjected to SDS-PAGE and Coomassie staining.

Kapβ2 mutants binding experiments: approximately 30 μg of GST-hnRNP A1-NLS, GST-hNRNP M-NLS and GST-M9M were immobilized on glutathione sepharose (Amersham, NJ, USA), followed by addition of 20 μg of Kapβ2 or Kapβ2 W460A/W730A mutant[1]. Samples were washed extensively and a quarter of each reaction was subjected to SDS-PAGE and Coomassie staining.

Subcellular localization of proteins in HeLa cells

MBP, MBP-hnRNP A1-NLS and MBP-M9M were subcloned into the modified pCS2-MT mammalian vector at Sal I and Not I sites. HeLa cells were maintained in DMEM (GIBCO

BRL, Gaithersburg, MD) with 10% fetal bovine serum (Gemini Bio-Products, West Sacramento, CA). Cells were grown on 12 mm coverslips placed in 24-well cell culture and transfected using Effectene (Qiagen, Valencia, CA) according to the manufacturer's instructions. After 16 hours, cells were fixed with 4% formaldehyde in PBS for 10 minutes at room temperature, permeabilized with 0.2% Triton X-100 in PBS for 5 minutes at room temperature, and blocked in 1%BSA/PBS. Cells were incubated with primary antibodies in 1% BSA/PBS for one hour at room temperature followed by secondary antibodies, and stained with 4,6-diamidino-2-phenylindole (DAPI). Goat-anti-myc-FITC polyclonal antibody (Bethyl Laboratories, Montgomery, TX) diluted to 5 ug/ml was used to detect the myc-MBP-peptides.

The monoclonal antibody 4C2 (a gift from Dr. M. Matunis) at 1:1000 dilution detected endogenous hnRNP A1 when incubated with goat-anti-mouse-Cy3 (Jackson ImmunoResearch Laboratories, West Grove, PA) antibody at 1:400 dilution. 4C2 has been previously shown to recognize human hnRNP A1, A2, B1 and B2[9]. We show by western blot (below) that 4C2 recognizes the hnRNP A1 fragment 257-305 but not the chimeric inhibitory peptide M9M (Supplementary Fig. 3). Monoclonal antibody 2A6 (a gift from Dr. M. Swanson) was used at 1:1000 dilution to detect endogenous hnRNP M. Mouse anti-HuR antibody was purchased from Zymed and was used at 1:100 dilution. HDAC1 has previously been reported to be imported into the nucleus by Kapα/Kapβ1[10]. We have confirmed by *in vitro* binding assays that recombinant HDAC1 binds Kapα but not Kapβ2 (data not shown). To detect endogenous HDAC1, mouse anti-HDAC1 monoclonal antibody 2E10 (Upstate Biotechnology; diluted 1:500) was used. Cells were then examined in a Zeiss Axiovert 200M microscope with De-convolution and Apotome systems. Images were acquired with the AxioVision software (Carl Zeiss Image Solutions) and processed with Image J software (National Institutes of Health, Bethesda, MD).

HuR and hnRNP M images were acquired using a Leica TCS SP5 confocal microscope and the Leica LAS AF software (Leica Microsystems Inc). 52-157 transfected cells were analyzed for each of the experiments, and percentages with cytoplasmic substrates are shown in a histogram (Figure 2d).

For western blot analysis, MBP-hnRNP A1-NLS, MBP-hnRNP M-NLS, MBP-M9M proteins or HeLa lysates were resolved on SDS-PAGE, transferred to PVDF membrane and probed with monoclonal antibody 4C2 diluted at 1:2000 and antibody 2A6 diluted at 1:1000. Secondary horseradish peroxidase-conjugated anti-mouse antibody (diluted 1:10000, Amersham) and the ECL system (Amersham) were used to visualize the blots.

References

1. Lee, B.J. et al. Cell 126, 543-58 (2006).
2. Chook, Y.M., Jung, A., Rosen, M.K. & Blobel, G. Biochemistry 41, 6955-6966 (2002).
3. Otwinowski, Z. & Minor, W. Methods in Enzymology 276, 307-326 (1997).
4. McCoy, A.J., Grosse-Kunstleve, R.W., Storoni, L.C. & Read, R.J. Acta Cryst. D61 , 458-464 (2005).
5. CCP4. Acta Crystallogr. D 50(1994).
6. Brunger, A.T. et al. Acta Cryst. A D54, 905-921 (1998).
7. Emsley, P. & Cowtan, K. Acta Crystallogr D Biol Crystallogr 60, 2126-32 (2004).
8. DeLano, W.L. (2002).
9. Matunis, M.J., Matunis, E.L. & Dreyfuss, G. J Cell Biol 116, 245-55 (1992).
10. Smillie, D.A., Llinas, A.J., Ryan, J.T., Kemp, G.D. & Sommerville, J. J Cell Sci 117, 1857-66 (2004).